RESEARCH ARTICLE



Rarasaponin-bentonite-activated biochar from durian shells composite for removal of crystal violet and Cr(VI) from aqueous solution

Livy Laysandra ¹ • Felix Harijaya Santosa ¹ • Vic Austen ^{1,2} • Felycia Edi Soetaredjo ¹ • Kuncoro Foe ³ • Jindrayani Nyoo Putro ⁴ • Yi-Hsu Ju ⁵ • Suryadi Ismadji ¹

Received: 26 June 2018 / Accepted: 28 August 2018 / Published online: 3 September 2018 © Springer-Verlag GmbH Germany, part of Springer Nature 2018

Abstract

This paper presents the preparation of composite material and its application for the adsorption of crystal violet and Cr(VI) from aqueous solution onto acid-activated bentonite (AAB) and rarasaponin–bentonite-activated biochar from durian shells composite (RBAB). The influence of initial pH of the solution and the temperature of adsorption on the adsorbents adsorption performance was also studied. Langmuir and Freundlich models could represent the adsorption equilibria equally well. Thermodynamic parameters such as ΔG° , ΔH° , and ΔS° were evaluated based on the adsorption isotherms. The values of ΔG° , ΔH° , and ΔS° for crystal violet adsorption system demonstrate behavior contrary to the Cr(VI) adsorption system. Where crystal violet adsorption is preferred at high temperatures with $q_{\rm max}$, value is 518.64 mg/L; while adsorption Cr(VI) is better at low temperature with $q_{\rm max}$, value is 106.30 mg/L. Pseudo-first-order and pseudo-second-order kinetic models could represent the kinetic data well.

Keywords Rarasaponin · Raw durian · Biochar · Composite · Isotherms · Kinetics · Adsorption

Introduction

Undoubtedly, the problem of heavy metal contaminants in groundwater, rivers, and lakes has become an impactful issue on human health. The increase of the waste produced by industries, coupled with the generally low awareness of the society, especially in the least developed countries, makes this environmental issue become a serious problem. One of the most common heavy metal contaminants found in water sources is chromate ions ($HCrO_4^-$ or $Cr_2O_7^{2-}$). Especially,

level of damage to the marine and other aquatic ecosystems (Cieslak-Golonka 1995; Zhitkovich et al. 2002; Albadarin et al. 2012).

Another type of contaminant that is harmful to the human

Cr(VI) ions are highly toxic, carcinogenic, mutagenic, and due to its relatively stable and soluble nature, it inflicts a high

Another type of contaminant that is harmful to the human and environment is organic dyes. This contaminant mostly comes from the coloring activities of many kinds of industries. One of the organic dyes widely used in many applications is crystal violet. Crystal violet is commonly applied in the

Responsible editor: Tito Roberto Cadaval Jr

Electronic supplementary material The online version of this article (https://doi.org/10.1007/s11356-018-3104-x) contains supplementary material, which is available to authorized users.

- Felycia Edi Soetaredjo felyciae@yahoo.com
- Suryadi Ismadji suryadiismadji@yahoo.com
- Department of Chemical Engineering, Widya Mandala Surabaya Catholic University, Kalijudan 37, Surabaya 60114, Indonesia
- Intan Permata Hati, Raya Kedung Baruk No.112 114, Surabaya 60298, Indonesia

- Widya Mandala Surabaya Catholic University, Pakuwon City, Kalisari 1, Surabaya 60112, Indonesia
- Department of Chemical Engineering, National Taiwan University of Science and Technology, No. 43, Sec 4, Keelung Rd, Da'an District, Taipei City 106, Taiwan
- Graduate Institute of Applied Science and Technology, National Taiwan University of Science and Technology, No. 43, Sec 4, Keelung Rd,. Da'an District, Taipei City 106, Taiwan



medical field such as for histological stains, bacteriostatic medicine, and skin disinfectants (Mittal et al. 2010). In the chemical industry, crystal violet is used to color textile and paper. Crystal violet is a useful dye from the industrial point of view. However, it is harmful when ingested, inhaled, or may cause skin irritation when exposed to bare skin and may cause permanent blindness when directly exposed to the eye (Ahmad 2009). Crystal violet and Cr(VI) are also found as by-products of some industries, such as paint making, leather tanning, battery manufacturing industries, and others (Jianmin et al. 2010; Zhang et al. 2012).

Among the many available methods for removing heavy metals and dyes from waterways, adsorption is one of the most effective, efficient, low-cost methods (Sahoo et al. 2005). The advantages of this process are the flexibility, and the effectiveness of the process can be adjusted by changing the adsorbents, 100% removal of a pollutant can be achieved for low concentration of pollutant, and ease of operation. The adsorption capacity of the adsorbent plays an important role in the success of the adsorption process. Therefore, a variety of adsorption studies have been conducted to find suitable adsorbents to remove these kinds of contaminants from water or wastewater.

Many of the studies have attempted to explore the possibility of using low-cost materials as the adsorbent for adsorbing heavy metals and dye contaminants, and also the optimum conditions for the preparation or production of those adsorbents. These low-cost adsorbents include natural bentonite (Hu et al. 2006; Karapinar and Donat 2009), bentonite modified with surfactant (Anirudhan and Ramachandran 2007; Chandra et al. 2013; Merino et al. 2016), biomasses (Febrianto et al. 2009; Kumar et al. 2009; Kurniawan et al. 2011a), activated carbon (Mohan et al. 2006; Al-Degs et al. 2008; Barkat et al. 2009; Chandra et al. 2009), or biochar (Chen et al. 2011; Zhang et al. 2013; Zhu et al. 2016; Dong et al. 2017). Each of these adsorbents has different adsorption characteristic and behavior. For industrial application, their availability in a large amount is one of the most important factors that need to be considered.

Natural bentonite is available abundantly in many parts of the world. The main constituent of this clay material is montmorillonite. It is a 2:1 aluminosilicate mineral in which an octahedral alumina sheet sandwiched between two tetrahedral silica sheets. The use of bentonite as the adsorbent is highly effective due to its modifiable property (Luckham and Rossi 1999). However, natural bentonite from some areas of the world has a low adsorption ability due to its impurities (Rahardjo et al. 2011). Removal of those impurities from the structure of bentonite will increase its adsorption ability (Eren and Afsin 2008).

Activated carbon has proven as a very effective adsorbent for the removal of various hazardous contaminants from water or wastewater (Purkait et al. 2007), although its downside is its high preparation cost and difficult regeneration process. The main problem to utilize activated carbon as an adsorbent for the wastewater treatment process is in its price; the commercial activated carbons are expensive. Therefore, many industries, especially in the developing countries, try to skip this costly process. To overcome the above problem, therefore, it is necessary to combine activated carbon with much cheaper materials to produce new adsorbent without losing its adsorption capability.

To the present, the literature about the study of preparation of bentonite-activated biochar composite and subsequent application of the result as the adsorbent for hazardous substance removal is rarely available. Therefore, the preparation of bentonite-activated biochar composite and its application for heavy metal and dye removal is the novelty of this paper. In this paper, preparation, characterization, and application of a new composite material called as rarasaponin–bentonite-activated biochar is presented. The composite material was made from durian shell, bentonite, and natural surfactant (rarasaponin). The composite was utilized for the adsorption of crystal violet and Cr(VI) from aqueous solution. The adsorption isotherms, kinetics, and thermodynamics aspects of the adsorption of Cr(IV) and crystal violet are given in this paper.

Materials and methods

Materials preparations

Preparation of acid-activated bentonite (AAB)

In this study, raw natural bentonite (RNB) was acquired from the bentonite excavation located in Pacitan, East Java, Indonesia. The type of the raw natural bentonite from this location was Ca-bentonite. The initial moisture content of RNB was 38.4%, and it was dried in an oven at 110 °C until its moisture content drops to 15-17%. The cation exchange capacity of RNB was 42.7 meg/100 g bentonite (determined according to ASTM C837-99). RNB was activated using 3 N of the H₂SO₄ solution with the ratio of RNB to the H₂SO₄ solution that was 1:5 (w/v). During the activation process, the mixture was heated at 60 °C under constant stirring at 400 rpm. After the activation process completed (1 h), the AAB was separated from the solution and placed in a sonicator and sonicated for 5 h at room temperature (32 °C). Subsequently, the AAB was washed several times using deionized water until the pH of the washing solution reached 6–7 (neutral). Afterward, the AAB was dried at 105 °C in the oven (Memmert UM 400). Dried AAB then crushed into a powder using a micro hammer mill (JANKE and KUNKEL) and sifted to obtain a particle size of – 180/+ 200 mesh using



vibration screener (Retsch AS-200). The AAB powder was stored in the desiccator until further used.

Preparation of rarasaponin

Rarasaponin was obtained from the extraction of *Sapindus rarak DC* (berry soap). The berry soap fruits were purchased from Klaten (Central Java, Indonesia). Details of the extraction procedure can be seen elsewhere (Kurniawan et al. 2011b).

Preparation of rarasaponin-bentonite

One gram of rarasaponin was dissolved in 100 mL of deionized water. Rarasaponin solution was mixed with AAB powder and then stirred at 800 rpm and 80 °C for 30 min. The ratio of AAB with the rarasaponin solution was 1:10 (w/v ratio). The solid was separated from the solution using centrifugation and dried using an oven at 105 °C. The dry rarasaponin—bentonite was crushed into a powder and sieved in vibration screen to obtain the particle size of -180/+200 mesh.

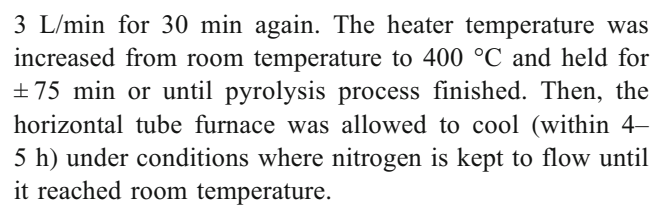
Preparation of durian shell

The waste of durian shell was collected from local durian processing industry in Surabaya. Durian shell waste is thoroughly rinsed using distilled water to remove the impurities and was cut into \pm 1 × 1 cm pieces and dried using the oven at 85 °C until the weight is constant. After the drying process completed, dried durian shell was crushed using a micro hammer mill into a powder with particle size of - 120/+ 140 mesh. Durian shells powder was stored in the desiccator for further used.

All inorganic chemicals used in this study ($K_2Cr_2O_7$, 1,5-diphenylcarbazide, NaOH, HCl, NaCl, H₃PO₄, H₂SO₄, and KOH) were purchased from Merck as analytical grade and directly used without any further treatment. Crystal violet (A.R. Grade, purity > 90%; chemical formula $C_{25}H_{30}Cl$; MW 407.98 g/mol), as a cationic dye, was purchased from Sigma–Aldrich, Singapore, and used without any further purification.

Preparation of rarasaponin-bentonite-activated biochar composite (RBAB)

Five grams of durian shell powder was placed into a cylinder tube and inserted in a horizontal tubular furnace (CARBOLITE GERO 21–503514). The nitrogen and carbon dioxide gas alternately flowed in the horizontal tubular furnace to create inert and oxidizing conditions, respectively. The system was run under nitrogen gas flow rate at 3 L/min for 30 min, then replaced by carbon dioxide at 3 L/min for 15 min, and finally flowed nitrogen at



To increase the porosity and to remove impurities from the biochar pore structure, activation using KOH was performed. The biochar powder and 1.65 M KOH solution were mixed with the ratio of 1:100 (w/v ratio). The mixture was stirred at 500 rpm and heated at 90 °C for 6 h. Then, the mixture was allowed to stand for 12 h, rinsed with distilled water until the pH of the washing solution reached 6-7, and dried overnight in an oven at 105 °C. The biochar activation process was conducted twice with the same procedure. Activated biochar was stored in airtight containers for further characterization and composite preparation. The preparation of composite from activated biochar from durian shell with rarasaponinbentonite was carried out under the similar procedure of mixing process of acid-activated bentonite and rarasaponin. The various mass ratios between activated biochar with rarasaponin-bentonite were 1:1, 1:2, 1:3, and 1:4. The composite production was conducted by microwave heating irradiation method at 700 W (National NN-S327 WF) for 4 min.

Characterization of adsorbents

The characterizations of the adsorbents were conducted via Fourier-transform infrared spectroscopy (FTIR), X-ray diffraction (XRD), and nitrogen sorption methods. FTIR spectroscopy was used to identify the functional groups of the adsorbents. Characterization of AAB and RBAB before and after the adsorption process was analyzed using FTIR SHIMADZU 8400S with KBr pellet method in the wavelength range of 400–4000/cm.

The X-ray diffraction analysis of the samples was performed on a Philips X'pert Xray Diffractometer. The radiation source used for the XRD analysis was a monochromatic high-intensity Cu Ka1 which has the wavelength (λ) of 0.15405 nm. The XRD patterns were acquired at 40 kV and 30 mA and temperature of 20 °C. The nitrogen sorption analysis of the samples was conducted at the boiling point of nitrogen gas (-196 °C) using Micromeritics ASAP 2010 sorption analyzer. The samples were degassed at high vacuum condition and temperature of 150 °C before measurements. The degassing of the samples was conducted for 24 h. The BET (Brunauer-Emmett-Teller) surface area was calculated at a range of relative pressure (p/p^{o}) of 0.05 to 0.25, while the total pore volume was obtained at the highest relative pressure (0.999). The surface topography of the samples was obtained using SEM analysis (JEOL



JSM-6500F). Before analysis, the samples were coated with a thin layer of platinum.

Adsorption experiments

For the adsorption isotherm studies, the removal of the crystal violet and Cr(VI) was conducted by two different types of adsorbents, AAB and RBAB. The adsorption experiment was carried out by adding the various mass adsorbent into a series of iodine flasks containing 50 mL of adsorbate solution at different temperatures (30, 50, 70 ± 0.5) °C. The iodine flasks containing adsorbents and adsorbate were placed in a thermostatic water-bath shaker (MEMMERT SV-1422) and shaken at 100 rpm for a certain time and a certain temperature. After the adsorption process completed, the solid was separated from the solution using a centrifuge at 4800 rpm for 10 min. The initial concentration and the equilibrium concentration of the adsorbate in the solution was measured quantitatively using a spectrophotometer (SHIMADZU UV/VIS-1700 PharmaSpec) at a certain maximum wavelength (590 nm for crystal violet and 543 nm for Cr(VI)). The concentration of Cr(VI) in the solution was determined using spectrophotometry technique, and the diphenylcarbazide method was employed. The influence of pH and adsorption time on the uptake of crystal violet and Cr(VI) were also examined. The sulfuric acid solution was used to adjust the pH of the solution.

The kinetics adsorption data were obtained at three different initial concentrations of crystal violet and Cr(VI). A similar procedure to the experimental adsorption isotherm was employed to collect the kinetic data. At a certain time interval, one iodine flask was taken from the system and the concentration of the adsorbate at time *t* was measured spectrophotometrically. All of the adsorption experiments (isotherm and kinetics) were conducted three times, and the average results are presented in this work.

The amount of adsorbate adsorbed by the adsorbents at equilibrium condition and at time t can be calculated using the following equations:

$$q_e = \frac{(C_o - C_i)}{m} \times V \tag{1}$$

$$q_t = \frac{(C_o - C_t)}{m} \times V \tag{2}$$

where C_o , C_i , and C_t (mg/L) are the initial concentrations, equilibrium concentration, and concentration of the adsorobate at time t, respectively. The symbol m represents the mass of adsorbent (g), and V is the volume of the solution (L).

Results and discussions

Physical and chemical characteristics of AAB and RBAB

To understand the adsorption mechanisms of Cr(VI) and CV onto AAB and RBAB, the FTIR analysis was carried out on AAB and RBAB. The FTIR analysis was conducted on pristine, Cr-loaded, and CV-loaded adsorbents. The FTIR analysis results for both adsorbents are summarized in supplementary material S1, and the FTIR spectra are given in Fig. 1.

Some distinctive functional groups of bentonite are found in both AAB and RBAB. The functional groups of the tetrahedral layers include the silanol group (Si-O-Si) stretch (wavenumber 1196/cm) and bend (wavenumber 440/cm), the Si-O stretch (wavenumber 810/cm) in quartz. Meanwhile, the octahedral group is represented by the Al-O-Si at wavenumber 648/cm and the O-H stretch (when bonded by $2Al^{3+}$) at wavenumber 918/cm.

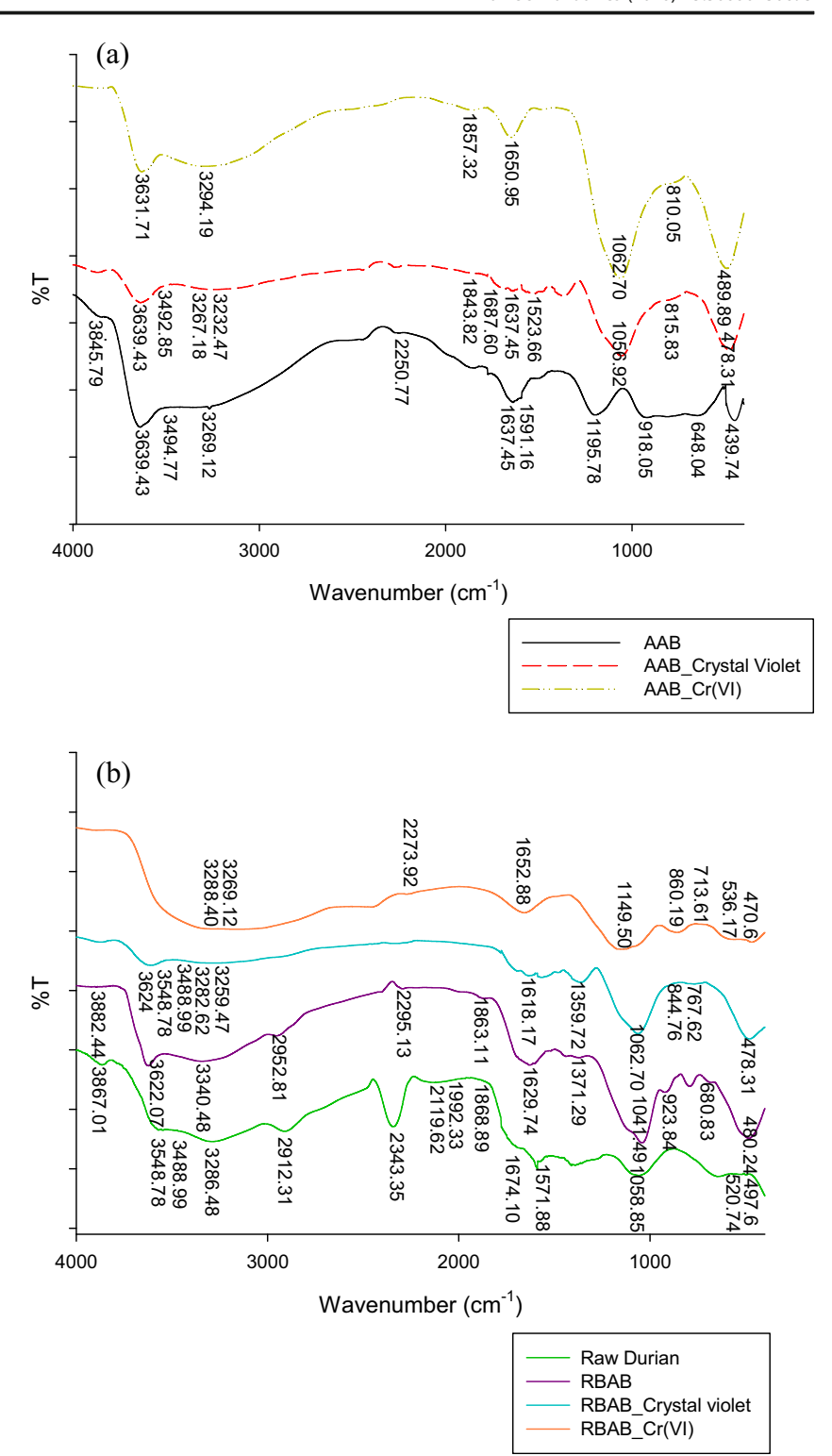
Since the rarasaponin was used as the surfactant in the composite preparation, the defining functional group of the rarasaponin (C=O stretch in deacylated carbonyl group, wavenumber 1371/cm) could be seen in all pristine RBAB, and Cr(VI) or crystal violet loaded RBAB. The addition of rarasaponin may also cause an alteration of the silanol band (from 1196 to 1041/cm) as seen in supplementary material S1 and Fig. 1. Intercalation of rarasaponin in the tetrahedral and octahedral layers of bentonite caused the alteration of this band.

The alteration in the silanol group also occurred when the adsorbents adsorbed Cr(VI) and crystal violet. For AAB, the silanol band originally was observed at wavenumber 1196/cm, and after the adsorption of crystal violet, the band alters to wavenumber 1057/cm, and for the adsorption of Cr(VI), this band alters to wavenumber 1063/cm. A similar phenomenon was also observed for the adsorption of crystal violet and Cr(VI) onto RBAB. The silanol band shifted from wavenumber 1041/cm to 1062/cm after loaded with crystal violet, and to 1150/cm after loaded with Cr(VI).

The X-ray diffraction patterns of durian shell, rarasaponin-bentonite, AAB, and RBAB are shown in Fig. 2. The XRD pattern of durian shell indicates that this material possesses both crystalline and amorphous structure. For acid-activated bentonite, the typical peaks of montmorillonite were observed in its XRD pattern. The characteristic peaks of montmorillonite were found in $2\theta = 6.52$, 20.22, 30.14, 35.18, and 60.16. The basal spacing at $2\theta = 6.52^{\circ}$ relates to $d_{001} = 1.354$ nm. The intercalation of natural surfactant, rarasaponin, increases this basal spacing into $d_{001} = 1.578$ nm (Fig. 2c). After combination with activated biochar from durian shell, the diffraction pattern of RBAB (Fig. 2d) indicates that the amorphous structure of activated biochar is more dominant than the montmorillonite structure. However, the main characteristic peak of



Fig. 1 FTIR result of **(a)** AAB and **(b)** RBAB



montmorillonite still can be observed at $2\theta = 5.46^{\circ}$, this value of 2θ corresponds to $d_{001} = 1.617$ nm.

The pore characteristics of the durian shell, rarasaponinbentonite, AAB, and RBAB are listed in Table 1. Low BET surface area and pore volume of durian shell indicate that this material possesses non-porous structure. Intercalation of rarasaponin into montmorillonite interlayer only slightly increases the BET surface area as seen in Table 1. However, due to the increase in interlayer spacing of montmorillonite, the pore volume of rarasaponin increased by almost 50% compared to the AAB. The combination of rarasaponin, bentonite, and activated biochar from durian shell to form composite



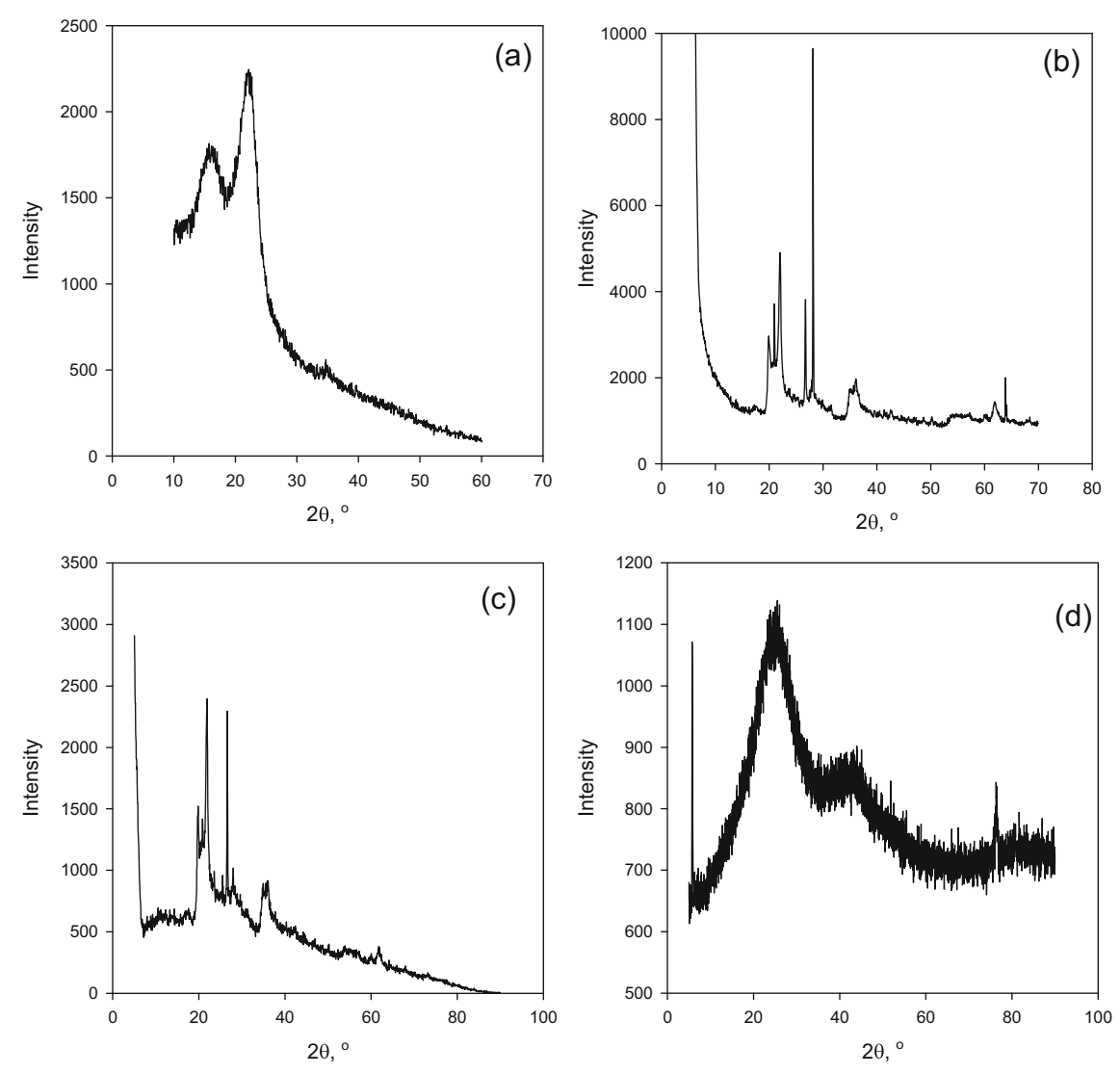


Fig. 2 XRD patterns of (a) durian shell, (b) AAB, (c) rarasaponin bentonite, and (d) RBAB composite

significantly increases the BET surface area and pore volume. The significant increase of the pore structure of the composite is due to the presence of a microporous structure in activated biochar.

The SEM analysis of the samples is given in the supplementary material S2. From this figure, it can be seen that the modification of AAB with rarasaponin did not change the surface morphology or topography of AAB. However, the

Table 1 The physical characteristic of the durian shell, rarasaponin-bentonite, AAB, and RBAB

Solid	BET, m ² /g	Pore volume (V_p) , cm ³ /g
Durian shell	1.89	0.002
AAB	71.8	0.124
Rarasaponin-bentonite	73.2	0.183
RBAB	402.6	0.394

incorporation of activated biochar changed the surface morphology of AAB. The change of surface morphology of the composite is possibly due to the different structures of AAB and biochar; the AAB is a mesoporous material, while the biochar is a microporous material.

Effect of initial pH on crystal violet and Cr(VI) adsorption

The adsorption capability of the raw materials (AAB, rarasaponin–bentonite, and biochar) and composites was tested for the removal of crystal violet and Cr(IV) from aqueous solution. The effect of KOH concentration used in the activation process on the removal performance of dye and heavy metal was also studied. Based on the experimental results (Table 2), 1.65 M KOH was selected for use in the biochar activation process for the preparation of RBAB.

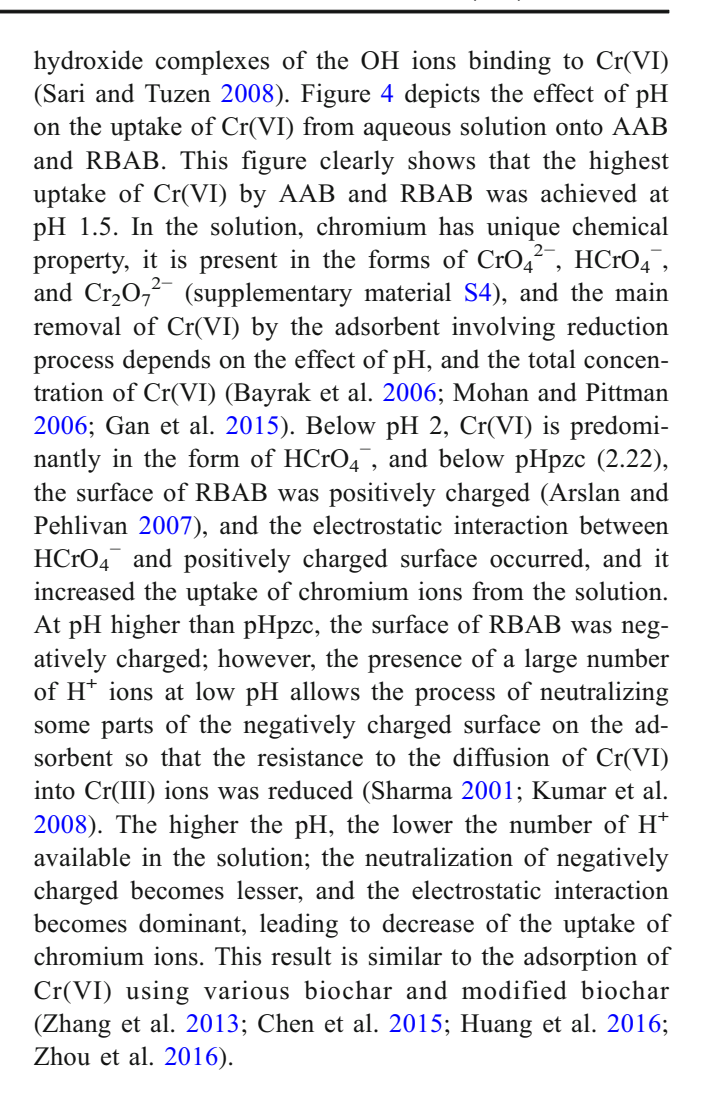


Table 2 Removal of crystal violet (Co = 800 ppm; pH = 7.0; t = 90 min, mass adsorbent = 0.5 g/L; and T = 30 °C) and Cr(VI) (Co = 400 ppm; pH = 1.5; t = 240 min; mass adsorbent = 0.5 g/L and T = 30 °C) by the adsorbents

Type of adsorbents	qe (mg/g)				
	Crystal violet	Cr(VI)			
Raw bentonite	5.6767	0.6804			
Acid activated bentonite (AAB)	79.2741	10.9704			
Rarasaponin-bentonite	79.7949	11.4865			
Biochar from durian shells	32.4074	6.6600			
Activated biochar from durian shell	s with KOH concentr	ration			
0.75 M	21.4175	0.8318			
1.05 M	24.0601	0.8841			
1.35 M	34.9647	2.4411			
1.65 M	51.4878	7.6110			
1.95 M	51.4769	7.5850			
The one-time activation process of a biochar using KOH (1.65 M) with	1	e-activated			
1:1	69.8547	17.9505			
1:2	78.1659	19.6016			
1:3	76.0587	19.5081			
1:4	75.8566	19.4025			
Two-time the activation process of rarasaponin–bentonite-activated biochar using KOH (1.65 M) with the mass ratio					
1:1	76.3962	19.7522			
1:2	80.1137	32.4488			
1:3	79.3365	23.4158			
1:4	78.7203	23.0240			

The pH at point zero charges (pHpzc) of the adsorbents was determined using the drift method (Lopez-Ramon et al. 1999; Prahas et al. 2008). The pHpzc AAB was 3.98 and 2.22 for RBAB (see supplementary material S3). Below pHpzc, the adsorbent is positively charged, while above pHpzc, the adsorbent is negatively charged. The initial solution pH is one of the crucial parameters that strongly influences the adsorption process of dyes and heavy metals. As can be seen in Fig. 3, it was found that the highest removal of Crystal violet was obtained at pH 9 (by AAC) and pH 8 (by RBAB). Crystal violet is a cationic dye, if the pH of the solution is below pHpzc, the repulsion interaction between the surface of adsorbent which was positively charged with crystal violet ions occurred, and this phenomenon retarded the uptake of dye molecules by the adsorbent. However, if the pH of the solution is above pHpzc, the electrostatic interaction between negatively charged surface of the adsorbent and positive ions of crystal violet occurred, and this electrostatic interaction enhanced the uptake of crystal violet dye onto the adsorbent.

In the adsorption of Cr(VI), the pH of the system should not exceed 7 (1.5–7.0) due to the formation of



Equilibrium adsorption isotherm studies

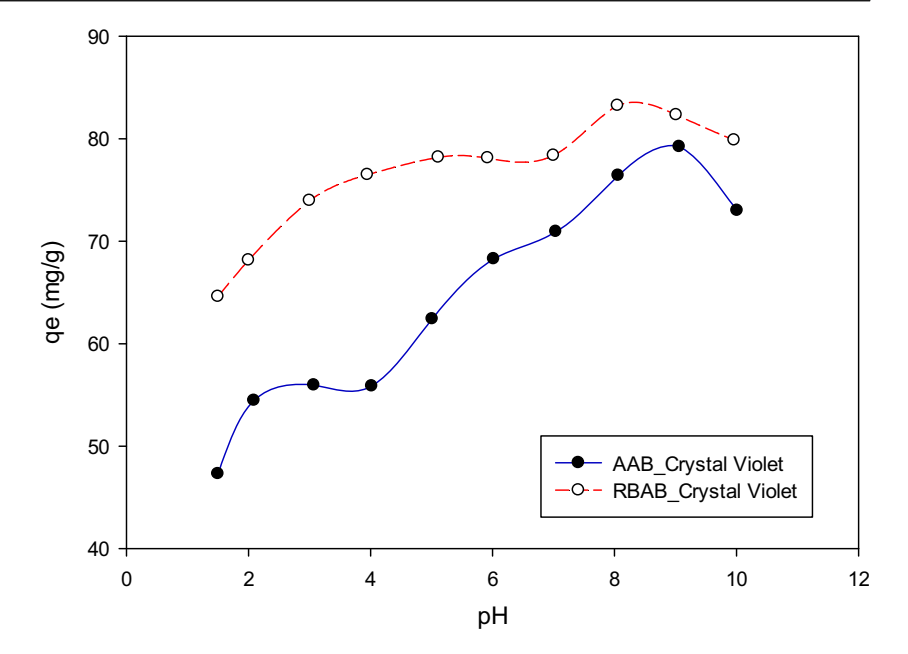
The adsorption equilibrium data for Cr(VI) ions and crystal violet onto AAB and RBAB were correlated with two isotherm models (Langmuir and Freundlich). The Langmuir equation is a widely used isotherm model to describe monolayer adsorption on a homogenous surface. This model assumes that an adsorbate only occupies one active site. Mathematically, the equation for the Langmuir model is given below (Langmuir 1918):

$$q_{\rm e} = q_{\rm m} \left(\frac{K_{\rm L} C_{\rm e}}{1 + K_{\rm L} C_{\rm e}} \right) \tag{3}$$

In this equation, q_e represents the amount of solute adsorbed in equilibrium conditions (mg/g), while C_e is representing the equilibrium concentration (mg/L). q_m denotes the maximum adsorption capability of the adsorbent. The K_L is a parameter known as the Langmuir equilibrium constant (L/g), which describes how strong the surface of the adsorbent can attract the adsorbate molecules.



Fig. 3 The effect of pH for adsorption crystal violet. Contact time = 90 min, Co = 800 ppm, T = 30 °C, mass adsorbent = 0.5 g/50 mL



The important characteristic of the Langmuir equation is $R_{\rm L}$ (dimensionless separation factor), which can be expressed as follows (Hall et al. 1966):

$$R_{\rm L} = \frac{1}{1 + K_{\rm L}C_{\rm e}} \tag{4}$$

The determination of the $R_{\rm L}$ value is used to predict whether the adsorption system is "favorable" or "unfavorable" (supplementary material S5).

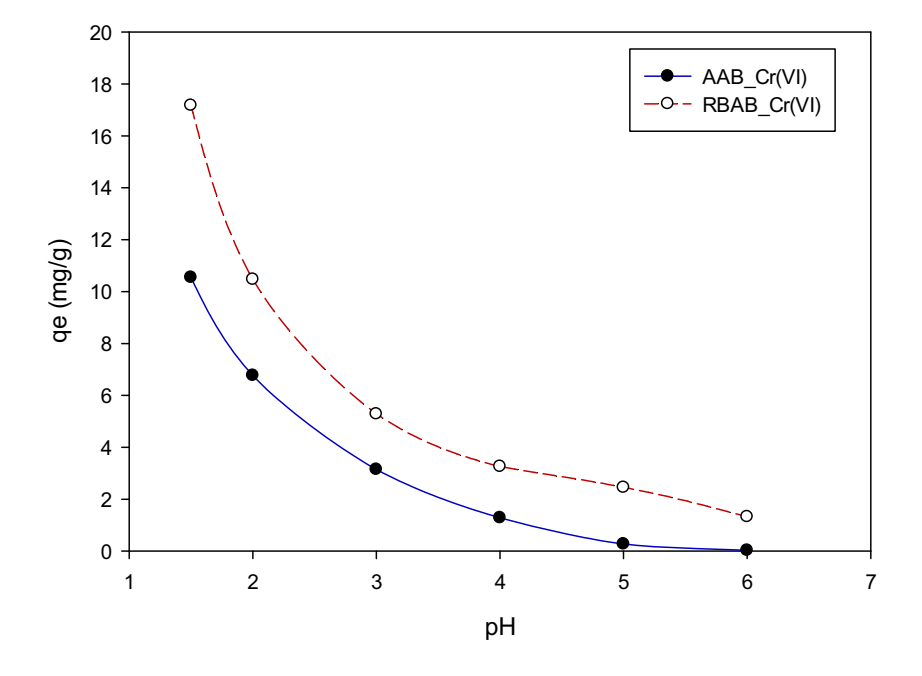
The other model used to correlate the experimental data is the Freundlich model, it is also a very prominent isotherm model with two parameters. This model is used to illustrate the adsorption behavior in heterogeneous systems. The Freundlich model can be expressed mathematically by the following equation (Sari and Tuzen 2008; Zheng et al. 2009):

$$q_{\rm m} = K_{\rm F} C_{\rm e}^{1/n_f} \tag{5}$$

where $K_{\rm F}$ and $n_{\rm f}$ are the Freundlich parameters which corresponds to the adsorption capacity [(mg/g)/(mg/L)^{1/n}] and heterogeneity factor, respectively. n_F is also known as adsorption intensity.

The adsorption isotherms of crystal violet and Cr(VI) onto AAB and RBAB at various temperatures are depicted in Figs. 5 and 6. The solid lines represent the theoretical values

Fig. 4 The effect of pH for the adsorption of Cr(VI) onto AAB and RBAB. Contact time = 4 h, Co = 300 ppm, T = 30 °C, mass adsorbent = 0.5 g/50 mL





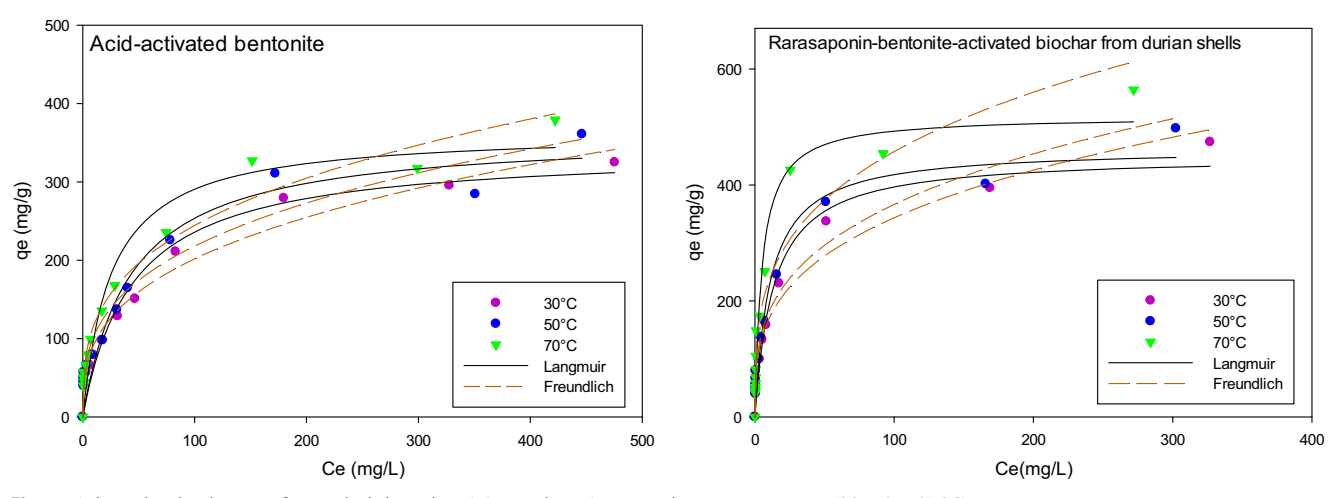


Fig. 5 Adsorption isotherms of crystal violet using AAB and RBAB at various temperatures (30, 50, 70) °C

of Langmuir isotherms, while the dash lines are the representation of the Freundlich equation. The parameters of Langmuir and Freundlich isotherm models obtained from the fitting of the experimental data are summarized in Table 3. Both of the models gave a high correlation coefficient ($r^2 > 0.90$) and indicate that both of the isotherms could represent the experimental adsorption data well. However, the judgment of the validity of the model should not only base on the high correlation coefficient but should consider the physical meaning of the parameters itself and reasonability of parameters' value.

The adsorption of crystal violet onto AAB and RBAB is an endothermic process as indicated by the uptake of the adsorbate increased with the increase of temperature. Consistent and reasonable values of the parameters of Langmuir and Freundlich are observed in Table 3. It is considered that the chemisorption process becomes dominant in this case. Parameters $q_{\rm max}$ and $K_{\rm L}$ of the Langmuir equation increase with the increase of temperature. For the endothermic process, the temperature has a positive influence on the uptake of the

solute; the amount adsorbed increases with the increase of temperature, and the parameter of $q_{\rm max}$ accommodates this phenomenon. The parameter K_L indicates how strong the adsorbent attracts the adsorbate molecules from the solution. For the endothermic process, the heat of adsorption is negative (the enthalpy of adsorption process is positive), the heat is required to attract the adsorbate and to enhance the uptake of the adsorbate by the adsorbent, and the increase of temperature will increase the attraction force between adsorbent and adsorbate molecules. The value of parameter K_L of Langmuir is consistent with this phenomenon.

Similar results were also observed for Freundlich isotherm, where the increased parameter values of K_F and n_f are also proportional to the temperature rise. The increase of the value of the parameter $n_{\rm f}$ expresses the deviation of the adsorption linearity, with the allowable value being $1 < n_f < 10$. The higher the value of $n_{\rm f}$ represents, the more heterogeneous the adsorbent surface. For the endothermic adsorption process, the heterogeneity of the system increases with the increase

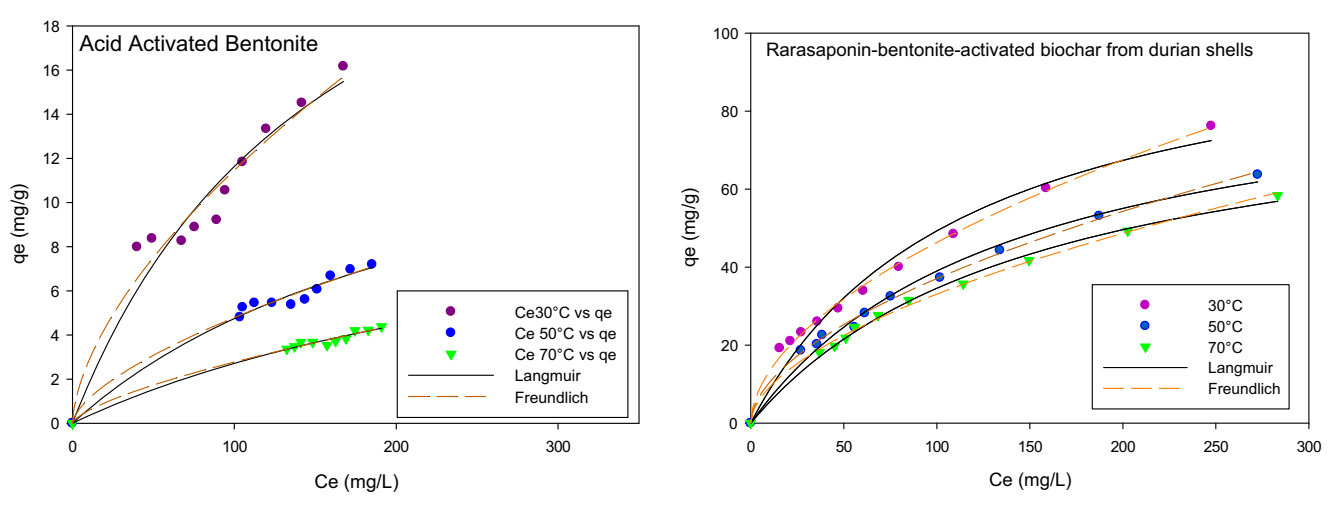


Fig. 6 Adsorption isotherms of Cr(VI) using AAB and RBAB at various temperatures (30, 50, 70) °C



Table 3 Langmuir and Freundlich parameters for the adsorption of crystal violet (Co = 800 mg/L; at pH 9 for AAB and 8 for RBAB) and Cr(VI) (Co for AAB = 200 mg/L and RBAB = 400 mg/L; at pH of 1.5) onto adsorbents at various temperatures

Adsorbate	Adsorbent at T (°C)	Langmuir parameters				Freundlich parameters		
		$q_{ m m}$ (mg/g)	K _L (L/mg)	$R_{ m L}$	R^2	Kf (mg/g)(mg/L) ⁻ⁿ)	$n_{ m f}$	r^2
Crystal violet	AAB							
	30	340.9212	0.0225	0.0526	0.9458	42.5936	2.9611	0.9810
	50		0.0235	0.0505		48.9308		
	70	361.6640	0.0393	0.0393	0.9261	56.3947	3.0803	0.9618
		364.6439			0.9402		3.1289	0.9782
	RBAB							
	30	450.1455	0.0741	0.0166	0.9526	82.7740	3.2360	0.9755
	50		0.0913	0.0135		88.6045		
	70	463.6654	0.1912	0.0065	0.9593	119.7423	3.2432	0.9663
		518.6415			0.9587		3.4340	0.9299
Cr(VI)	AAB							
	30	30.4232	0.0062	0.4464	0.9443	0.6903	1.6385	0.9613
	50	16.5199	0.0040	0.5556	0.9796	0.2548	1.5699	0.9814
	70	12.1273	0.0029	0.6329	0.9889	0.1199	1.4633	0.9894
	RBAB							
	30	106.3005	0.0087	0.3650	0.9734	3.7927	1.8397	0.9973
	50	93.7067	0.0071	0.4132	0.9889	2.9094	1.8098	0.9971
	70	87.7863	0.0065	0.4348	0.9958	2.5309	1.7917	0.9971

of temperature. A consistent result of parameter $n_{\rm f}$ of Freundlich equation with the physical meaning of the parameter is observed in Table 3.

The adsorption of Cr(VI) from the solution onto AAB and RBAB was an exothermic process and expresses physical adsorption, and the uptake of Cr(VI) decreased with increasing temperature (Fig. 6). The parameters of Langmuir and Freundlich obtained from the fitting of the experimental adsorption data are also consistent with the phenomena for physical adsorption as seen in Table 3. These results confirm that both Langmuir and Freundlich could represent the experimental adsorption data well for the adsorption of crystal violet and Cr(VI) onto AAB and RBAB. Furthermore, the value of $R_{\rm L}$ of Langmuir equation was found in the range of 0.0526–0.0065. Hence, the adsorption of crystal violet or Cr(VI) by AAB and RBAB is both favorable.

The adsorption capacity of RBAB (for both adsorption of crystal violet and Cr(VI)) is higher than the adsorption capability of AAB. The higher adsorption capacity of RBAB than AAB due to higher BET surface area of RBAB than AAB is seen in Table 2. The pore structure of RBAB is the combination of micropore and mesopore. With the presence of micropore, more active adsorption sites are available; the interaction between the active sites and adsorbate molecules becomes higher, and more adsorbate molecules were adsorbed onto the surface of AAB. Furthermore, the presence of several functional groups of biochar in the surface of RBAB such as

O–H stretch, etc. enhanced the uptake of crystal violet and Cr(VI). The comparison of adsorption capacity between RBAB and other adsorbents to remove crystal violet and Cr(VI) is presented in Table 4. The high adsorption capacity of RBAB is promising as the adsorbent for removal crystal violet and Cr(IV) from water or wastewater.

Thermodynamics of adsorption

The thermodynamic properties of the adsorption process can be obtained from the adsorption equilibria at various temperatures. The thermodynamic properties of the adsorption process are Gibbs free energy change ΔG° (kJ/mol), standard enthalpy change ΔH° (kJ/mol), and standard entropy change ΔS° (J/mol). The thermodynamic properties of the adsorption of crystal violet and Cr(VI) were calculated using the following equations:

$$In K_{\rm D} = \frac{\Delta S^{\circ}}{R} - \frac{\Delta H^{\circ}}{R} \cdot \frac{1}{T} \tag{6}$$

$$\Delta G^{\circ} = RT \operatorname{In} K_{D} \tag{7}$$

where R is the ideal gas constant (8.31434 J/mol/K), T is the absolute temperature (K), and K_D is the linear sorption distribution coefficient. The value of K_D can be obtained through a



 Table 4
 The comparison of adsorption capacity of various adsorbents with AAB and RBAB for the removal of crystal violet and Cr(VI)

Adsorbate	Adsorbent	Operational condition			Adsorption capacity (mg/g)	References	
			pH T (°C)		capacity (mg/g)		
Crystal violet	Artocarpus heterophyllus (jackfruit) leaf powder	7	20	120	43.398	(Saha et al. 2012)	
·			30		41.651		
			40		37.434		
	Ananas comosus (pineapple) leaf powder	8	20	180	78.227	(Chakraborty et al. 2012)	
			30		75.176		
			40		72.391		
	Fugas sawdust cartoon	6	25	-	78.69	(Aljeboree 2016)	
	Activated carbon	7	30	1440	271.0	(Sewu et al. 2017)	
	Rice straw biochar				620.3		
	Korean cabbage biochar				1304		
	Wood chip biochar	0	70	00	195.6	In this seeds	
	AAB RBAB	9 8	70	90	364.64	In this study	
C _m (VII)		2.0	40	90	518.64 1.422	(Warra et al. 2007)	
Cr(VI)	Spent activated clay	2.5	40	90	0.649	(Weng et al. 2007)	
		3.0			0.557		
		3.5			0.548		
		4.0			0.334		
	Oak wood char	2.0	25	_	3.031	(Mohan et al. 2011)	
	Ouk wood Char	2.0	35		4.076	(Worldin et al. 2011)	
			45		4.930		
	Oak bark char		25		4.619		
	Our our one		35		7.433		
			45		7.515		
	Bone char	1	_	120	8.4	(Hyder et al. 2015)	
	Cashew nuts shell	5	25	60	8.421	(Coelho et al. 2014)	
	Activated coal				9.933	(Coomo et an 2011)	
	Micelle-clay	6	25	180	9.43	(Qurie et al. 2013)	
	Natural clay	1	20	_	3.61	(Akar et al. 2009)	
	HDTMA modified with clay	•	20		10.18	(i iiiii et iii 2007)	
	Durian peel	2	_	30	10.67	(Saueprasearsit 2011)	
	Kaolinite	4.6	30	240	11.6	(Bhattacharyya and Sen 2006	
	Acid-activated kaolinite				13.9	`	
	ZrO-kaolinite				10.9		
	TBA-kaolinite				10.6		
	Coconut shell charcoal:	5.2	_	180		(Babel and Kurniawan 2004)	
	As received				2.1820		
	Coated with chitosan				3.6519		
	Oxidized with sulfuric acid				4.0503		
	Oxidized with sulfuric and				8.9476		
	coated with chitosan						
	Oxidized with nitric acid				10.8762		
	Commercial activated carbon:						
	As received				4.7216		
	Oxidized with sulfuric acid				8.9449		
	Oxidized with nitric acid				10.4373		
	Natural Algerian bentonite	5	20	120	12.61	(Barkat et al. 2014)	
	Activated carbon	2.0	25	120	38.17	(Abdel et al. 2012)	
	Bentonite	_			48.83		
	Cross-linked chitosan/bentonite composite	2	25	240	89.13	(Liu et al. 2015)	
		4			37.92		
		7		100	18.78		
	Activated carbon	2.0	25	120	38.17	(Abdel et al. 2012)	
	Bentonite			2.15	48.83		
	Cross-linked chitosan/bentonite composite	2	25	240	89.13	(Liu et al. 2015)	
		4			37.92		
	AAD	7	20	240	18.78	T 411 4 1	
	AAB	1.5	30	240	30.4232	In this study	
	RBAB				106.3005		



Table 5 Thermodynamic properties of the adsorption of crystal violet and Cr(VI) onto AAB and RBAB

Type of adsorbent	Type of adsorbate	T(K)	ΔG° (kJ/mol)	ΔH° (kJ/mol)	ΔS° (J/mol)
AAB	Crystal violet	303	- 6.2780	25.4490	104.7765
	Cr(VI)	323 343	- 8.4396 - 10.4633	-40.9813	-150.4646
		303	4.4408		
		323	7.2250		
		343	10.4108		
RBAB	Crystal violet	303	-12.5660	8.7451	70.2936
	Cr(VI)	323 343	- 13.9739 - 15.3793	- 12.2385	-41.4561
		303	1.2087		
		323	1.3954		
		343	1.5959		

straight line plot of ln (qe/Ce) versus Ce and extrapolate to zero Ce. The values of standard enthalpy change (ΔH°) and standard entropy change (ΔS°) were obtained from the plot of Eq. (6) as given in the supplementary material S6. The thermodynamic properties of the adsorption of crystal violet and Cr(VI) are summarized in Table 5.

In the adsorption system of crystal violet by both adsorbents at three different temperatures (30, 50, and 70 °C), the positive value of enthalpy change (ΔH°) was obtained and indicates that the adsorption of crystal violet ions onto AAB and RBAB is an endothermic process. This result is in accordance with the experimental

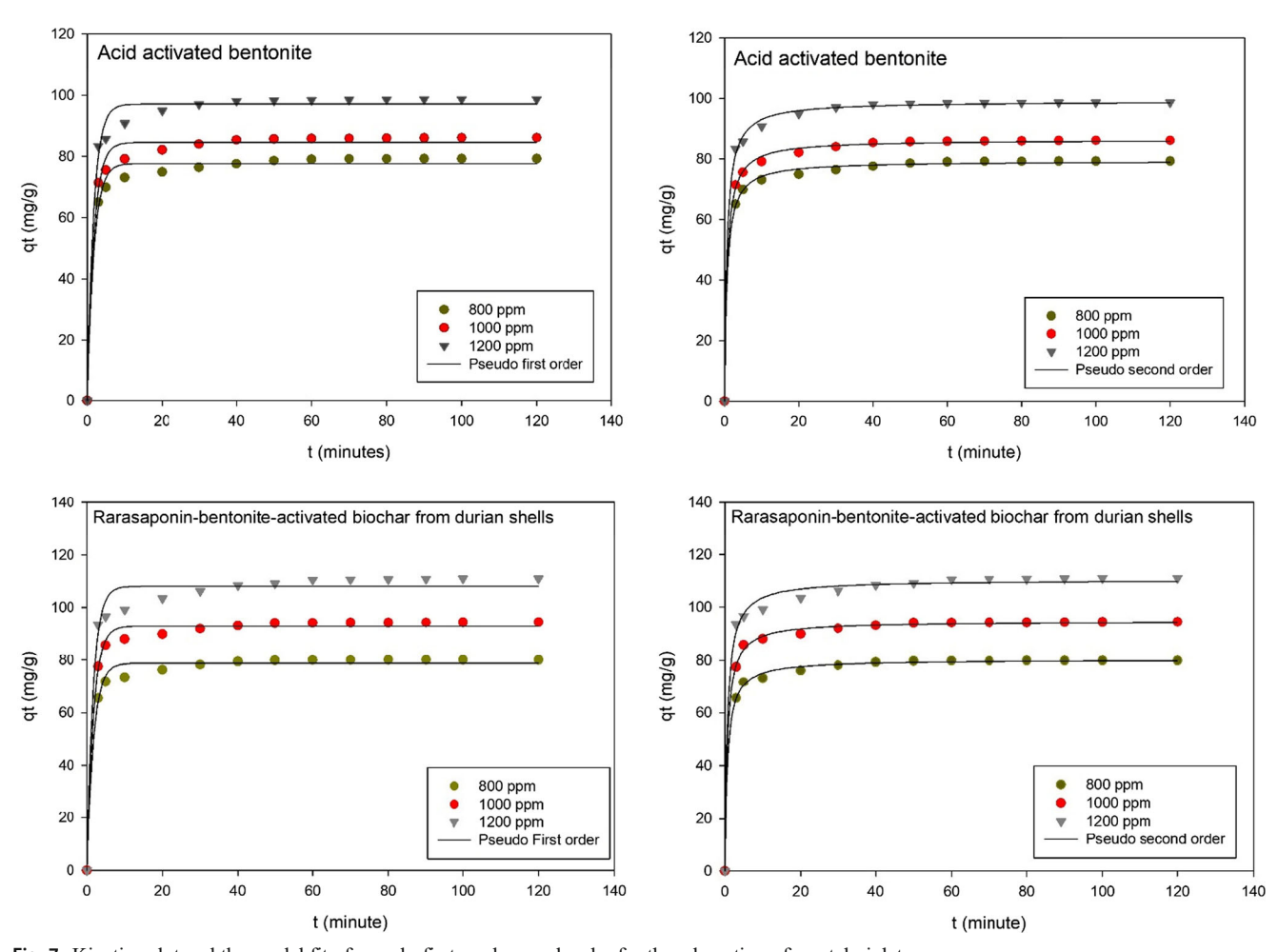


Fig. 7 Kinetics plot and the model fit of pseudo-first- and second-order for the adsorption of crystal violet

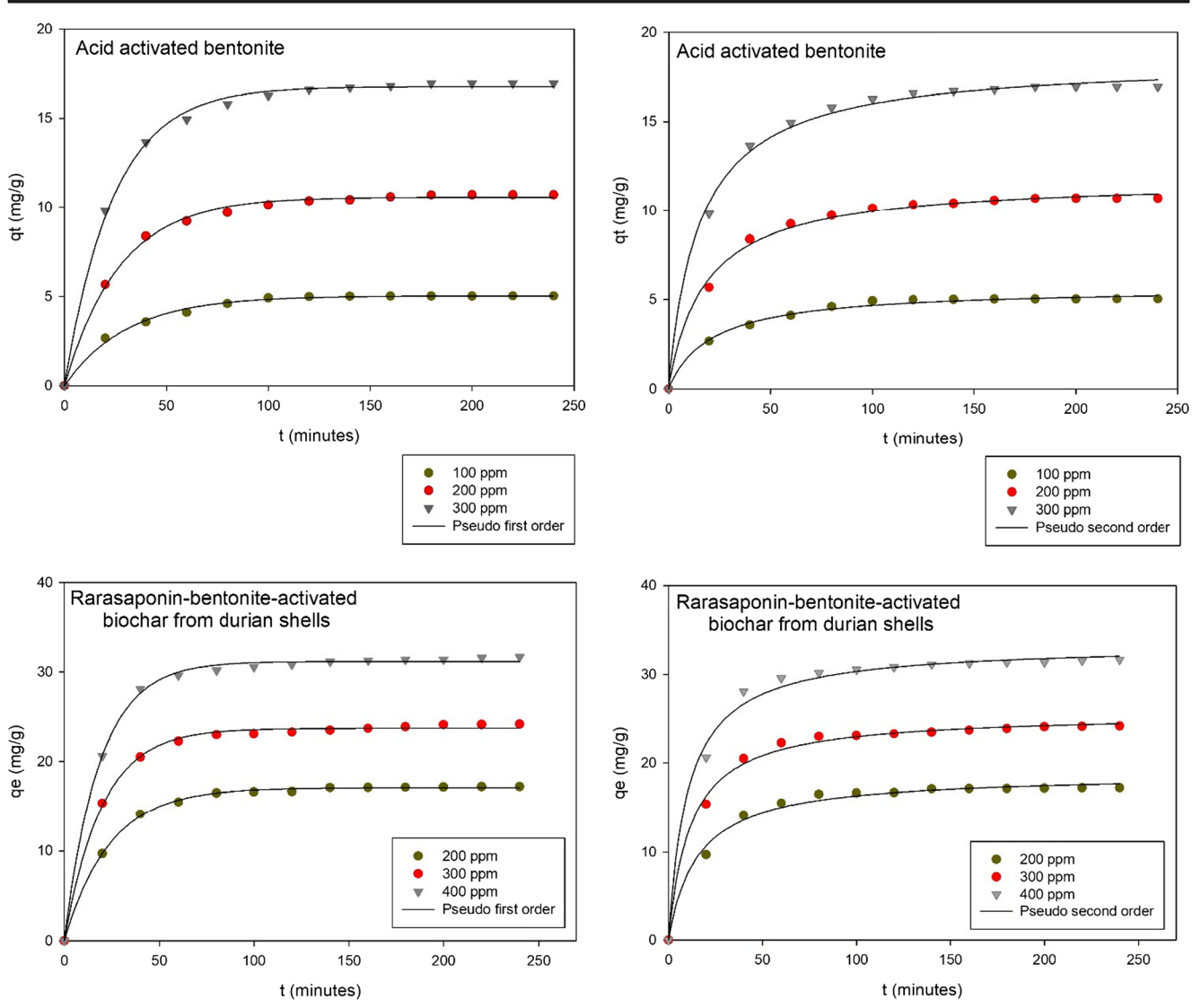


Fig. 8 Kinetics plot and the model fit of pseudo-first- and second-order for the adsorption of Cr(VI)

adsorption isotherms. The negative values of Gibb's free energy change (ΔG°) at all temperatures indicate that the adsorption process is spontaneous and more favorable at high temperatures. The standard entropy change (ΔS°) measures the randomness of the adsorption system. If the value of $\Delta S^{\circ} > 0$, then there is an increase in the randomness of the adsorption system due to the high affinity of the adsorbate molecule against the active site of the adsorbent (Singha and Das 2013).

Meanwhile, the thermodynamic behavior in the solid/liquid adsorption system of Cr(VI) by both types of adsorbent has the opposite properties, as shown in Table 5. The ΔG° values > 0, which suggest that the adsorption of Cr(VI) is nonspontaneous and requires a small amount of energy. In this case, the adsorption process occurs naturally. The negative value of the standard enthalpy change (ΔH°) indicates that the adsorption process is exothermic. Negative values of ΔS°

represent a stable arrangement (low randomness) of Cr(VI) on both AAB and RBAB surfaces.

Adsorption kinetics

To examine the kinetic mechanisms in the adsorption process, the pseudo-first-order and pseudo-second-order kinetic models were used to test the validity of the kinetic adsorption experimental data of crystal violet and Cr(VI) by AAB and RBAB. The pseudo-first-order equation of Lagergren (Zhang et al. 2013) is presented as:

$$q_{\rm t} = q_{\rm el}(1 - \exp(-k_{\rm 1ad}t))$$
 (8)

where q_t is the amount of adsorbate adsorbed at time t (mg/g), $k_{1\text{ad}}$ is the pseudo-first-order reaction rate constant (/min), and t is the time (min). On the other hand, pseudo-second-order



Table 6 Pseudo-first-order and pseudo-second-order kinetic parameters for adsorption of crystal violet and Cr(VI) onto AAB and RBAB at various initial concentrations

Adsorbate	Initial concentration of crystal violet (ppm)	Experimental result	Pseudo-first-order			Pseudo-second-order		
		$qe_{\rm exp}~({\rm mg/g})$	k_{lad} (/min)	q _{e1} (mg/g)	r^2	k_{2ad} (mg/g/min)	q _{e2} (mg/g)	r_2^2
Crystal violet	AAB				,			
	800	79.2741	0.5574	77.7509	0.9903	0.0182	79.3701	0.9986
	1000	86.1758	0.5616	84.6694	0.9897	0.0168	86.4282	0.9988
	1200	98.6100	0.5787	97.0852	0.9884	0.0155	99.0415	0.9984
	RBAB							
	800	79.9420	0.5583	78.7182	0.9913	0.0181	80.3374	0.9986
	1000	94.5062	0.5707	92.9895	0.9938	0.0164	94.7627	0.9988
	1200	111.0122	0.5977	108.0630	0.9824	0.0138	110.3855	0.9951
Cr(VI)	AAB							
	100	5.0341	0.0325	5.0348	0.9948	0.0082	5.6710	0.9921
	200	10.6997	0.0372	10.5596	0.9971	0.0047	11.7685	0.9953
	300	16.9532	0.0415	16.7700	0.9976	0.0035	18.4464	0.9961
	RBAB							
	200	17.2091	0.0420	17.0747	0.9990	0.0035	18.7578	0.9912
	300	24.1619	0.0505	23.7018	0.9977	0.0034	25.5960	0.9955
	400	31.6345	0.0545	31.1503	0.9984	0.0030	33.3983	0.9931

kinetic can be expressed in the following mathematical form (Ho and McKay 1999):

$$q_{\rm t} = q_{\rm e2} \left(\frac{q_{\rm e2} k_{\rm 2ad} t}{1 + q_{\rm e2} k_{\rm 2ad}} \right) \tag{9}$$

where k_{2ad} is the pseudo-second-order equilibrium rate constant (g/mg/min).

The experimental kinetic data and theoretical plots of the kinetic models for the adsorption of crystal violet and Cr(VI) onto AAB and RBAB are given in Figs. 7 and 8. The parameters of pseudo-first-order and pseudo-second-order equations are summarized in Table 6. Visually, both of the models could represent the experimental kinetic data well as seen in Figs. 7 and 8. The high correlation coefficient for both models is obvious as seen in Table 6. To judge the applicability of both models, the parameters obtained from the fitting of the experimental data should be observed further. The values of the parameters must be in accordance with the physical meaning of each parameter.

From Table 6, it can be seen that the value of the parameter $q_{\rm e2}$ is closer to the $q_{\rm exp}$ than the parameter $q_{\rm e1}$ of pseudo-first-order. Since the experimental data follows the pseudo-second-order kinetic model, the chemisorption controlled the adsorption of crystal violet onto AAB and RBAB. In contrast, the adsorption of Cr(VI) followed the pseudo-first-order model (Table 6), and the physical adsorption controlled the uptake of Cr(VI) by AAB and RBAB. The evidence of the adsorption isotherms supported both of these phenomena.

The initial concentration of the adsorbate gave significant influence on the equilibrium time. The higher the initial concentration, the longer time required to reach the equilibrium condition as indicated by parameters $k_{1\rm ad}$ and $k_{2\rm ad}$. Parameters $k_{1\rm ad}$ and $k_{2\rm ad}$ are time-scaling factors, an increase of the value of these parameters resulting shorter time required by the adsorption system to reach equilibrium. From Table 6, it can be seen that the pseudo-second-order gave the consistent value of $k_{2\rm ad}$ with its physical meaning, while the pseudo-first-order failed to give the consistent value of $k_{1\rm ad}$ with its physical meaning.

Conclusion

The new composite material was prepared from agricultural waste (durian shell), bentonite, and natural surfactant (rarasaponin). The FTIR, XRD, and nitrogen sorption analysis were employed for the characterization of the composite. The presence of a microporous structure in the composite enhances the BET surface area. The composite material was tested for its adsorption capability for liquid phase adsorption of crystal violet and Cr(VI). The results of this study indicated that RBAB could be effectively used as a new composite adsorbent for the removal of crystal violet and Cr(VI) from aqueous solutions. Temperature has a significant influence on the amount of uptake of adsorbates. The adsorption of crystal violet onto AAB and RBAB was an endothermic process,



while the exothermic process was observed for the adsorption of Cr(VI). Both of Langmuir and Freundlich adsorption isotherms could represent the experimental data well. The pseudo-second-order represents the kinetic data well for the adsorption of crystal violet, while the pseudo-first-order could describe the experimental data for adsorption of Cr(VI). The thermodynamic properties of adsorption such as ΔH° , ΔG° , and ΔS° were obtained from the adsorption isotherms at three different temperatures.

Funding Financial support is from the Ministry of Research and Technology and Higher Education through competency grant 2018.

References

- Abdel S, Monem A, Ahmed M et al (2012) Adsorption studies on the removal of hexavalent chromium-contaminated wastewater using activated carbon and bentonite. Chem J 2:95–105
- Ahmad R (2009) Studies on adsorption of crystal violet dye from aqueous solution onto coniferous pinus bark powder (CPBP). J Hazard Mater 171:767–773. https://doi.org/10.1016/j.jhazmat.2009.06.060
- Akar ST, Yetimoglu Y, Gedikbey T (2009) Removal of chromium (VI) ions from aqueous solutions by using Turkish montmorillonite clay: effect of activation and modification. Desalination 244:97–108. https://doi.org/10.1016/j.desal.2008.04.040
- Albadarin AB, Mangwandi C, Al-Muhtaseb AH et al (2012) Kinetic and thermodynamics of chromium ions adsorption onto low-cost dolomite adsorbent. Chem Eng J 179:193–202. https://doi.org/10.1016/j. cei.2011.10.080
- Al-Degs YS, El-Barghouthi MI, El-Sheikh AH, Walker GM (2008) Effect of solution pH, ionic strength, and temperature on adsorption behavior of reactive dyes on activated carbon. Dyes Pigments 77: 16–23. https://doi.org/10.1016/j.dyepig.2007.03.001
- Aljeboree AM (2016) Adsorption of crystal violet dye by Fugas sawdust from aqueous solution. Int J ChemTech Res 9:412–423
- Anirudhan TS, Ramachandran M (2007) Surfactant-modified bentonite as adsorbent for the removal of humic acid from wastewaters. Appl Clay Sci 35:276–281. https://doi.org/10.1016/j.clay.2006.09.009
- Arslan G, Pehlivan E (2007) Batch removal of chromium(VI) from aqueous solution by Turkish brown coals. Bioresour Technol 98:2836–2845. https://doi.org/10.1016/j.biortech.2006.09.041
- Babel S, Kurniawan TA (2004) Cr(VI) removal from synthetic wastewater using coconut shell charcoal and commercial activated carbon modified with oxidizing agents and/or chitosan. Chemosphere 54: 951–967. https://doi.org/10.1016/j.chemosphere.2003.10.001
- Barkat M, Chegrouche S, Mellah A, Bensmain B, Nibou D, Boufatit M (2014) Application of Algerian bentonite in the removal of cadmium (II) and chromium (VI) from aqueous solutions. J Surf Eng Mater Adv Technol 4:210–226. https://doi.org/10.4236/jsemat.2014.44024
- Barkat M, Nibou D, Chegrouche S, Mellah A (2009) Kinetics and thermodynamics studies of chromium(VI) ions adsorption onto activated carbon from aqueous solutions. Chem Eng Process Process Intensif 48:38–47. https://doi.org/10.1016/j.cep.2007.10.004
- Bayrak Y, Yesiloglu Y, Gecgel U (2006) Adsorption behavior of Cr(VI) on activated hazelnut shell ash and activated bentonite. Microporous Mesoporous Mater 91:107–110. https://doi.org/10.1016/j.micromeso.2005.11.010
- Bhattacharyya KG, Sen GS (2006) Adsorption of chromium(VI) from water by clays. Ind Eng Chem Res 45:7232–7240. https://doi.org/10.1021/ie060586j

- Chakraborty S, Chowdhury S, Das SP (2012) Insight into biosorption equilibrium, kinetics and thermodynamics of crystal violet onto Ananas comosus (pineapple) leaf powder. Appl Water Sci 2:135–141. https://doi.org/10.1007/s13201-012-0030-9
- Chandra I, Ju Y, Ayucitra A, Ismadji S (2013) Evans blue removal from wastewater by rarasaponin-bentonite. Int J Environ Sci Technol 10: 359–370
- Chandra TC, Mima MM, Sunarso J, Sudaryanto Y, Ismadji S (2009) Activated carbon from durian shell: preparation and characterization. J Taiwan Inst Chem Eng 40:457–462. https://doi.org/10.1016/j.jtice.2008.10.002
- Chen T, Zhou Z, Xu S, Wang H, Lu W (2015) Adsorption behavior comparison of trivalent and hexavalent chromium on biochar derived from municipal sludge. Bioresour Technol 190:388–394. https://doi.org/10.1016/j.biortech.2015.04.115
- Chen X, Chen G, Chen L, Chen Y, Lehmann J, McBride MB, Hay AG (2011) Adsorption of copper and zinc by biochars produced from pyrolysis of hardwood and corn straw in aqueous solution. Bioresour Technol 102:8877–8884. https://doi.org/10.1016/j.biortech.2011.06.078
- Cieslak-Golonka M (1995) Toxic report and mutagenic effects of chromium(VI) a review. Polyhedron 15:3667–3689. https://doi.org/10.1016/0277-5387(96)00141-6 1996
- Coelho GF, Gonçalves AC Jr, Tarley CRT et al (2014) Removal of metal ions Cd (II), Pb (II), and Cr (III) from water by the cashew nut shell Anacardium occidentale L. Ecol Eng 73:514–525. https://doi.org/ 10.1016/j.ecoleng.2014.09.103
- Dong H, Deng J, Xie Y, Zhang C, Jiang Z, Cheng Y, Hou K, Zeng G (2017) Stabilization of nanoscale zero-valent iron (nZVI) with modified biochar for Cr(VI) removal from aqueous solution. J Hazard Mater 332:79–86. https://doi.org/10.1016/j.jhazmat.2017.03.002
- Eren E, Afsin B (2008) An investigation of Cu(II) adsorption by raw and acid-activated bentonite: a combined potentiometric, thermodynamic, XRD, IR, DTA study. J Hazard Mater 151:682–691. https://doi. org/10.1016/j.jhazmat.2007.06.040
- Febrianto J, Kosasih AN, Sunarso J, Ju YH, Indraswati N, Ismadji S (2009) Equilibrium and kinetic studies in adsorption of heavy metals using biosorbent: a summary of recent studies. J Hazard Mater 162: 616–645. https://doi.org/10.1016/j.jhazmat.2008.06.042
- Gan C, Liu Y, Tan X, Wang S, Zeng G, Zheng B, Li T, Jiang Z, Liu W (2015) Effect of porous zinc-biochar nanocomposites on Cr(VI) adsorption from aqueous solution. RSC Adv 5:35107–35115. https://doi.org/10.1039/c5ra04416b
- Hall KR, Eagleton LC, Acrivos A, Vermeulen T (1966) Pore- and solid-diffusion kinetics in fixed-bed adsorption under constant-pattern conditions. Ind Eng Chem Fundam 5:212–223. https://doi.org/10.1021/i160018a011
- Ho YS, McKay G (1999) Pseudo-second order model for sorption processes. Process Biochem 34:451–465. https://doi.org/10.1016/S0032-9592(98)00112-5
- Hu QH, Qiao SZ, Haghseresht F, Wilson MA, Lu GQ (2006) Adsorption study for removal of basic red dye using bentonite. Ind Eng Chem Res 45:733–738. https://doi.org/10.1021/ie050889y
- Huang X, Liu Y, Liu S, Tan X, Ding Y, Zeng G, Zhou Y, Zhang M, Wang S, Zheng B (2016) Effective removal of Cr(VI) using β-cyclodex-trin-chitosan modified biochars with adsorption/reduction bifuctional roles. RSC Adv 6:94–104. https://doi.org/10.1039/C5RA22886G
- Hyder AHMG, Begum SA, Egiebor NO (2015) Adsorption isotherm and kinetic studies of hexavalent chromium removal from aqueous solution onto bone char. J Environ Chem Eng 3:1329–1336. https:// doi.org/10.1016/j.jece.2014.12.005
- Jian-min R, Si-wei W, Wei J (2010) Adsorption of crystal violet onto BTEA- and CTMA-bentonite from aqueous solutions. World Acad Sci Eng Technol 41:790–795



- Karapinar N, Donat R (2009) Adsorption behaviour of Cu²⁺and Cd²⁺onto natural bentonite. Desalination 249:123–129. https://doi.org/10. 1016/j.desal.2008.12.046
- Kumar R, Bishnoi NR, Garima BK (2008) Biosorption of chromium(VI) from aqueous solution and electroplating wastewater using fungal biomass. Chem Eng J 135:202–208. https://doi.org/10.1016/j.cej. 2007.03.004
- Kumar R, Singh R, Kumar N, Bishnoi K, Bishnoi NR (2009) Response surface methodology approach for optimization of biosorption process for removal of Cr (VI), Ni (II) and Zn (II) ions by immobilized bacterial biomass sp. Bacillus brevis. Chem Eng J 146:401–407. https://doi.org/10.1016/j.cej.2008.06.020
- Kurniawan A, Kosasih AN, Febrianto J, Ju YH, Sunarso J, Indraswati N, Ismadji S (2011a) Evaluation of cassava peel waste as lowcost biosorbent for Ni-sorption: equilibrium, kinetics, thermodynamics and mechanism. Chem Eng J 172:158–166
- Kurniawan A, Sutiono H, Ju YH, Soetaredjo FE, Ayucitra A, Yudha A, Ismadji S (2011b) Utilization of rarasaponin natural surfactant for organo-bentonite preparation: application for methylene blue removal from aqueous effluent. Microporous Mesoporous Mater 142:184–193. https://doi.org/10.1016/j.micromeso.2010.11.032
- Langmuir I (1918) The adsorption of gases on plane surfaces of glass, mica and platinum. J Am Chem Soc 40:1361–1403. https://doi.org/10.1021/ja02242a004
- Liu Q, Yang B, Zhang L, Huang R (2015) Adsorptive removal of Cr(VI) from aqueous solutions by cross-linked chitosan/bentonite composite. Korean J Chem Eng 32:1314–1322. https://doi.org/10.1007/s11814-014-0339-1
- Lopez-Ramon MV, Stoeckli F, Moreno-Castilla C, Carrasco-Marin F (1999) On the characterization of acidic and basic surface sites on carbons by various techniques. Carbon 37:1215–1221. https://doi.org/10.1016/S0008-6223(98)00317-0
- Luckham PF, Rossi S (1999) The colloidal and rheological properties of bentonite suspensions. Adv Colloid Interf Sci 82:43–92. https://doi. org/10.1016/S0001-8686(99)00005-6
- Merino D, Ollier R, Lanfranconi M, Alvarez V (2016) Preparation and characterization of soy lecithin-modified bentonites. Appl Clay Sci 128:17–22. https://doi.org/10.1016/j.clay.2016.04.006
- Mittal A, Mittal J, Malviya A, Kaur D, Gupta VK (2010) Adsorption of hazardous dye crystal violet from wastewater by waste materials. J Colloid Interface Sci 343:463–473. https://doi.org/10.1016/j.jcis. 2009.11.060
- Mohan D, Pittman CU (2006) Activated carbons and low cost adsorbents for remediation of tri- and hexavalent chromium from water. J Hazard Mater 137:762–811. https://doi.org/10.1016/j.jhazmat. 2006.06.060
- Mohan D, Rajput S, Singh VK, Steele PH, Pittman CU Jr (2011) Modeling and evaluation of chromium remediation from water using low cost biochar, a green adsorbent. J Hazard Mater 188: 319–333. https://doi.org/10.1016/j.jhazmat.2011.01.127
- Mohan D, Singh KP, Singh VK (2006) Trivalent chromium removal from wastewater using low cost activated carbon derived from agricultural waste material and activated carbon fabric cloth. J Hazard Mater 135:280–295. https://doi.org/10.1016/j.jhazmat.2005.11.075
- Prahas D, Kartika Y, Indraswati N, Ismadji S (2008) Activated carbon from jackfruit peel waste by H3PO4chemical activation: pore structure and surface chemistry characterization. Chem Eng J 140:32–42. https://doi.org/10.1016/j.cej.2007.08.032
- Purkait MK, Maiti A, DasGupta S, De S (2007) Removal of Congo red using activated carbon and its regeneration. J Hazard Mater 145: 287–295. https://doi.org/10.1016/j.jhazmat.2006.11.021

- Qurie M, Khamis M, Manassra A, Ayyad I, Nir S, Scrano L, Bufo SA, Karaman R (2013) Removal of Cr (VI) from aqueous environments using micelle-clay adsorption. Sci World J 2013:1–7. https://doi.org/10.1155/2013/942703
- Rahardjo AK, Susanto MJJ, Kurniawan A, Indraswati N, Ismadji S (2011) Modified Ponorogo bentonite for the removal of ampicillin from wastewater. J Hazard Mater 190:1001–1008. https://doi.org/ 10.1016/j.jhazmat.2011.04.052
- Saha PD, Chakraborty S, Chowdhury S (2012) Batch and continuous (fixed-bed column) biosorption of crystal violet by Artocarpus heterophyllus (jackfruit) leaf powder. Colloids Surfaces B Biointerfaces 92:262–270. https://doi.org/10.1016/j.colsurfb.2011. 11.057
- Sahoo C, Gupta AK, Pal A (2005) Photocatalytic degradation of crystal violet (C.I. Basic violet 3) on silver ion doped TiO2. Dyes Pigments 66:189–196. https://doi.org/10.1016/j.dyepig.2004.09.003
- Sari A, Tuzen M (2008) Biosorption of total chromium from aqueous solution by red algae (Ceramium virgatum): equilibrium, kinetic and thermodynamic studies. J Hazard Mater 160:349–355. https:// doi.org/10.1016/j.jhazmat.2008.03.005
- Saueprasearsit P (2011) Adsorption of chromium (Cr+6) using durian peel. 2011. Int Conf Biotechnol Environ Manag IPCBEE 18:33–38
- Sewu DD, Boakye P, Woo SH (2017) Highly efficient adsorption of cationic dye by biochar produced with Korean cabbage waste. Bioresour Technol 224:206–213. https://doi.org/10.1016/j.biortech. 2016.11.009
- Sharma YC (2001) Adsorption of Cr (VI) onto wollastonite: effect of pH. Indian J Chem Technol 8:186–190
- Singha B, Das SK (2013) Adsorptive removal of Cu(II) from aqueous solution and industrial effluent using natural/agricultural wastes. Colloids Surfaces B Biointerfaces 107:97–106. https://doi.org/10. 1016/j.colsurfb.2013.01.060
- Weng C, Sharma YC, Chu S (2007) Adsorption of Cr (VI) from aqueous solutions by spent activated clay. J Hazard Mater 155:65–75. https://doi.org/10.1016/j.jhazmat.2007.11.029
- Zhang W, Mao S, Chen H, Huang L, Qiu R (2013) Pb (II) and Cr (VI) sorption by biochars pyrolyzed from the municipal wastewater sludge under different heating conditions. Bioresour Technol 147: 545–552. https://doi.org/10.1016/j.biortech.2013.08.082
- Zhang Y, Li Y, Li J, Sheng G, Zhang Y, Zheng X (2012) Enhanced Cr(VI) removal by using the mixture of pillared bentonite and zero-valent iron. Chem Eng J 185–186:243–249. https://doi.org/10.1016/j.cej. 2012.01.095
- Zheng H, Liu D, Zheng Y, Liang S, Liu Z (2009) Sorption isotherm and kinetic modeling of aniline on Cr-bentonite. J Hazard Mater 167: 141–147. https://doi.org/10.1016/j.jhazmat.2008.12.093
- Zhitkovich A, Quievryn G, Messer J, Motylevich Z (2002) Reductive activation with cysteine represents a chromium(III)-dependent pathway in the induction of genotoxicity by carcinogenic chromium(VI). Environ Health Perspect 110:729–731. https://doi.org/10.1289/ehp. 02110s5729
- Zhou L, Liu Y, Liu S, Yin Y, Zeng G, Tan X, Hu X, Hu X, Jiang L, Ding Y, Liu S, Huang X (2016) Investigation of the adsorption-reduction mechanisms of hexavalent chromium by ramie biochars of different pyrolytic temperatures. Bioresour Technol 218:351–359. https://doi.org/10.1016/j.biortech.2016.06.102
- Zhu N, Yan T, Qiao J, Cao H (2016) Adsorption of arsenic, phosphorus and chromium by bismuth impregnated biochar: adsorption mechanism and depleted adsorbent utilization. Chemosphere 164:32–40. https://doi.org/10.1016/j.chemosphere.2016.08.036

